Green Chemistry

Cite this: *Green Chem.*, 2012, **14**, 1064

www.rsc.org/greenchem

PAPER

Cu–ZrO_2 nanocomposite catalyst for selective hydrogenation of levulinic acid and its ester to γ-valerolactone†

Amol M. Hengne and Chandrashekhar V. Rode*

Received 3rd December 2011, Accepted 12th January 2012
DOI: 10.1039/c2gc16558a

Several copper based catalysts were prepared, characterized and evaluated for the hydrogenation of levulinic acid and its methyl ester. Among these, nanocomposites of Cu–ZrO_2 and Cu–Al_2O_3 quantitatively catalyzed the hydrogenation of levulinic acid and its methyl ester to give 90–100% selectivity to γ-valerolactone in methanol and water respectively. Both the Cu–ZrO_2 and Cu–Al_2O_3 nanocomposites were prepared by the co-precipitation method using mixed precursors under controlled conditions. XRD results showed that the main active phase of the reduced Cu–ZrO_2 catalyst was metallic copper and particle size was found to be of 10–14 nm by HRTEM. The active metal leaching was at a maximum for the Cu–Al_2O_3 catalyst in a water medium due to the formation of a copper–carboxylate complex that was blue in colour. Surprisingly, copper leaching was completely suppressed in the case of the Cu–ZrO_2 catalyst in methanol in spite of the substrate loading was increased from 5 to 20% w/w. The excellent recyclability of the Cu–ZrO_2 catalyst with complete LA conversion and >90% GVL selectivity makes it a sustainable process having a commercial potential.

Introduction

'Biorefinery' is a sustainable way to produce both fuels and chemicals from bio-feedstock in an integrated complex.[1] In the first decade of 21st century, much research has been aimed at developing new catalytic routes for the conversion of several biobased platform molecules into fuels and multiple commodity products.[2] Oxygen present in the bioderived molecules poses an interesting challenge of selective hydro-deoxygenation by designing appropriate catalyst systems and at the same time would require less number of processing steps as compared to the fossil derived hydrocarbons.[3] Among various bio-feedstock options, abundantly available lignocellulosic material at lower cost can be easily converted to a variety of starting materials. For example, hydrolysis of cellulose in the presence of aqueous as well as alcoholic solutions gives levulinic acid (LA) and/or esters, for which other processes have already been developed which start from wood and agro wastes.[1,4] Downstream processing of LA gives several useful molecules and one of these is γ-valerolactone (GVL), obtained by the catalytic hydrogenation of LA. GVL is a sustainable commodity chemical having great commercial importance due to its applications as a solvent in lacquers, as a food additive and can be converted to a variety of monomers. It is also considered as a potential fuel additive for replacing ethanol in gasoline–ethanol blends.[3–5]

GVL synthesis from LA involves the first step of hydrogenation to give an intermediate, 4-hydroxy levulinic acid followed by its subsequent cyclization either by homogeneous or heterogeneous catalysts. Recently, a process for GVL from LA with high yields was reported using homogeneous catalysts such as $Ru(acac)_3$ in combination with TPPTS and water soluble homogeneous ruthenium with sulfonated triphenylphosphine ligands.[6,7] Homogeneous catalyst systems obviously have serious drawbacks of catalyst recovery and recycling, in addition to the multistep synthesis of ligands, thus they are far from the commercial application. Heterogeneous catalyst systems reported for the hydrogenation of LA include platinum oxide as well as chromium containing copper catalysts at 250 °C and 202 bar H_2 pressure with much longer reaction times of 44 h giving complex mixtures of products.[8,9] Other noble metals studied for LA hydrogenation are Pd, Ru, and Re. LA hydrogenation has been also studied in supercritical CO_2 over Ru–alumina and Ru–silica catalysts giving 99% conversion with complete selectivity to GVL under severe conditions of temperature and pressure (200 °C and 200 bar H_2).[10] Yan *et al.* have reported liquid-phase hydrogenation of LA to GVL over 5% Ru–C in a batch reactor giving 99% selectivity to GVL at 92% LA conversion. However, activity and stability of Ru–C catalyst was not reproducible in subsequent catalyst recycles due to substantial active metal leaching.[11] Lange *et al.* also observed serious problem of active metal leaching/deactivation of the heterogeneous catalyst in the hydrogenation of LA. Although carbon supports overcome the problem of leaching to some extent, but do not allow the regeneration of the deactivated catalyst.[12,13] Braden *et al.* reported a combination of two different noble metals (Ru–Re) with very high (15%) metal loading, in spite of which the conversion was

Chemical Engineering and Process Development Division, National Chemical Laboratory, Pune 411008, India. E-mail: cv.rode@ncl.res.in; Fax: +91 20 2590 2621; Tel: +91 20 2590 2349

†Electronic supplementary information (ESI) available: See DOI: 10.1039/c2gc16558a

restricted to only 15–40%.[14] Deng *et al.* attempted transfer hydrogenation of LA over two different Ru catalysts, using 4.5 MPa H_2 in the second step giving 88% yield of GVL.[15] Recently, Du *et al.* studied Au supported ZrO_2 catalyst for the transfer hydrogenation of LA with 99% selectivity to GVL however, reuse and stability of the catalyst was not studied.[16] Similar studies were carried out using homogeneous as well as heterogeneous Ru based catalysts, however, substantial leaching of the precious metal was observed.[17]

The potential commercial application of the LA hydrogenation to GVL process can thus be possible by developing a two part strategy *viz.* (i) a route which eliminates/minimizes the active metal leaching; and (ii) developing a non-noble metal catalyst for improved process economics. In the present work we demonstrate for the first time, the efficiency of non-noble Cu–ZrO_2 and Cu–Al_2O_3 catalysts for the hydrogenation of LA to GVL. Between the two catalysts, metal leaching in water was substantially reduced (Cu leaching, 34 ppm) for Cu–ZrO_2 catalyst due to stable tetragonal phase formation of ZrO_2 which strongly binds to the active Cu as compared to Cu–Al_2O_3 (Cu leaching, 174 ppm). The extent of metal leaching in case of Cu–ZrO_2 was almost completely suppressed (Cu leaching < 2 ppm) in methanol solvent, due to *in situ* formation of methyl levulinate, used as a substrate for its subsequent hydrogenation to GVL. Hence, the catalyst reuse was also possible for three times unlike Ru based catalysts.[11] Our copper based catalyst will thus have significant potential for commercial development since the lignocellulose decomposition is increasingly carried out in presence of alcohol to enhance overall yield of LA ester as compared to LA, due to substantial reduction in humin formation.[18]

Results and discussion

As the Cu–ZrO_2 catalyst showed the highest performance and stability for the hydrogenation of LA and its methyl ester, a detailed characterization of Cu–ZrO_2 was carried out and the results were also compared with those of other Cu based catalysts studied in this work.

The BET surface area of Cu–ZrO_2 was found to be 22.1 m^2 g^{-1} with a pore volume of 0.06 cc g^{-1} and a pore size of 2.7 nm (ESI, Table 1†). The microporous nature of the material was confirmed by a type IV adsorption isotherm (ESI, Fig. 1†).

XRD patterns of activated and used Cu–ZrO_2 catalyst samples are shown in Fig. 1(A). The appearance of indexed diffraction lines at 2θ = 43.5° (111), 50.6° (200), 60.2° (202) and 74.3° (220) indicate the presence of the crystalline phases of metallic Cu in all the samples.[19] The particle size evaluated from the Scherrer equation using the peak at 2θ = 43.50° having maximum intensity was found to be 13.5 nm, which matched very well with the HRTEM results. XRD results showed that the main active phase of the reduced Cu–ZrO_2 catalyst was metallic copper and a peak at 2θ = 30.5° (particle size = 8 nm) indicated the tetragonal phase of zirconia.[19,20] While the sample recovered after the reaction carried out in water, showed the intact metallic copper phase as evidenced by a peak at 2θ = 43.5°, however, the appearance of a new peak at 2θ = 36.5° indicated the formation of Cu_2O as shown in Fig. 1A(c). The extent of Cu metal and Cu_2O was evaluated as 67% and 33% respectively from the XPS

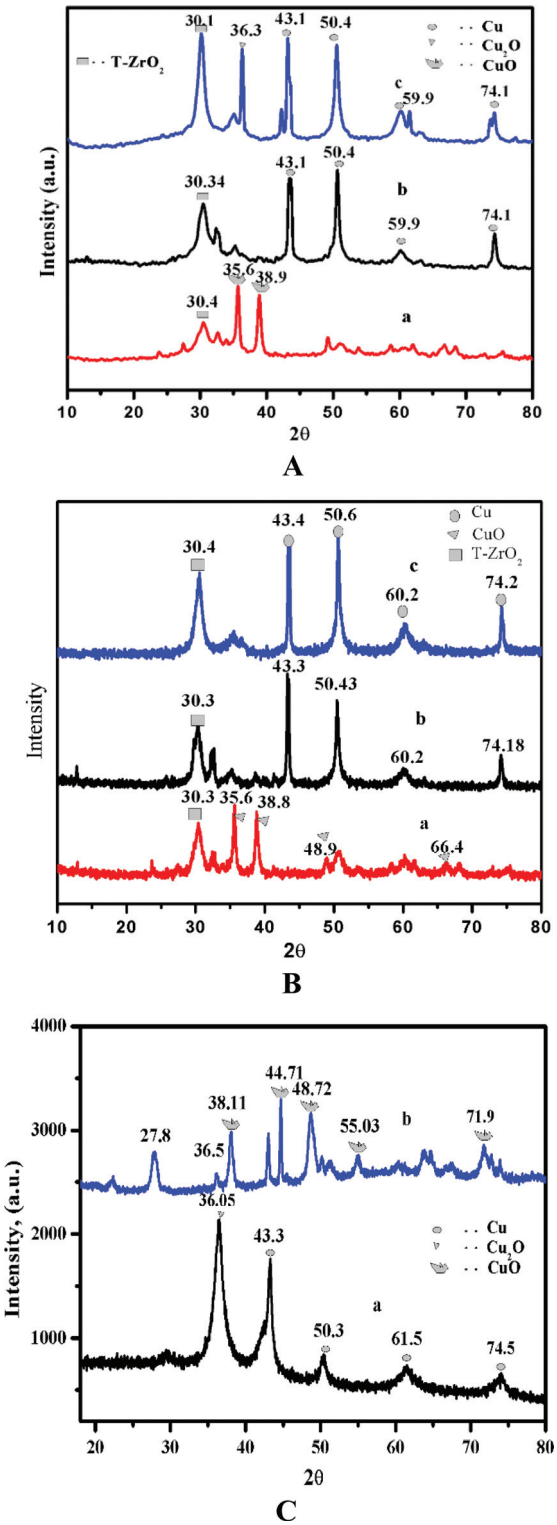

Fig. 1 (A) XRD patterns for nano Cu–ZrO_2 catalyst (a) calcined Cu–ZrO_2 (b) activated Cu–ZrO_2, and (c) used Cu–ZrO_2 in water. (B) XRD patterns for nano Cu–ZrO_2 catalyst (a) calcined Cu–ZrO_2 (b) activated Cu–ZrO_2, and (c) used Cu–ZrO_2 in methanol. (C) XRD patterns for nano Cu–Al_2O_3 catalyst (a) activated Cu–Al_2O_3 , and (b) used Cu–Al_2O_3 in water.

results (ESI, Fig. 2†). The increased sharpness of the peak at 2θ = 30.5° in the used sample, could be due to the increase in

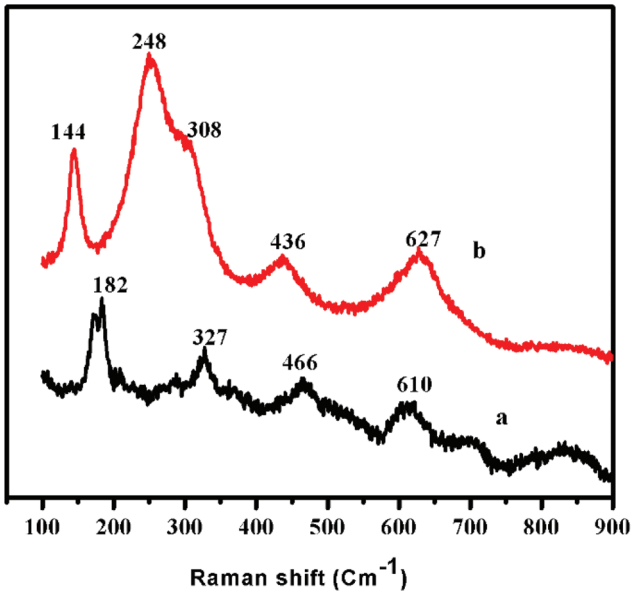

Fig. 2 Raman study of nano Cu–ZrO_2 catalyst (a) activated Cu–ZrO_2 (b) used Cu–ZrO_2 in water.

crystallite size (from 8 to 11 nm) of ZrO_2. In contrast to this, XRD of Cu–ZrO_2 recovered from the methanol medium (Fig. 1B) showed the presence of a metallic copper phase without any characteristic peak of Cu_2O.

XRD pattern of activated Cu–Al_2O_3 catalyst in Fig. 1(C) showed the presence of metallic copper and Cu_2O phases at 2θ = 43.5° (111) and 2θ = 36.5° respectively. However, in contrast to Cu–ZrO_2, both these phases disappeared in the recovered Cu–Al_2O_3 sample and the appearance of new peaks at 2θ = 38.1°, 44.7°, 48.72°, 71.9° and 27.8° indicated the presence of CuO and alumina phases respectively. This also explains the lower stability of Cu–Al_2O_3 catalyst as shown by the catalyst reuse studies discussed later.

In the Raman spectra of freshly activated (Fig. 2A) and recovered (Fig. 2B) Cu–ZrO_2 catalyst samples, weak and strong bands at 144, 436 and 627 cm^{-1} could be assigned to tetragonal ZrO_2, which was in accordance with the XRD results. In addition, the bands at 248 and 308 cm^{-1} were of surface CuO due to the exposure of the sample to air.[20] Although these bands in the recovered sample shifted to new values nevertheless, these are characteristics of the tetragonal ZrO_2 phase which is in good agreement with the XRD results. The absence of sharp bands in the Raman spectra of the recovered sample indicates the semi-crystalline nature due to its exposure to reaction conditions.[20]

Fig. 3(A) and (B) show NH_3-TPD profiles and Py-IR respectively, for various copper catalysts. Among these catalysts, Cu–Al_2O_3 and Cu–ZrO_2 showed broad peaks of NH_3 desorption in a high temperature region of 500–700 °C, indicating the presence of strong acid sites, while the other two catalysts (Cu–Cr_2O_3 and Cu–BaO) did not show any NH_3 desorption peaks indicating the absence of detectable acid sites. In order to distinguish between the acid sites, Py-IR of both Cu–ZrO_2 and Cu–Al_2O_3 samples were also studied which showed distinct peaks at 1539 and 1558 cm^{-1} due to mixed Lewis–Brønsted and only Brønsted acid sites respectively. The strong acidity of Cu–ZrO_2 evidenced by NH_3-TPD and Py-IR, resulted into its higher activity for acid

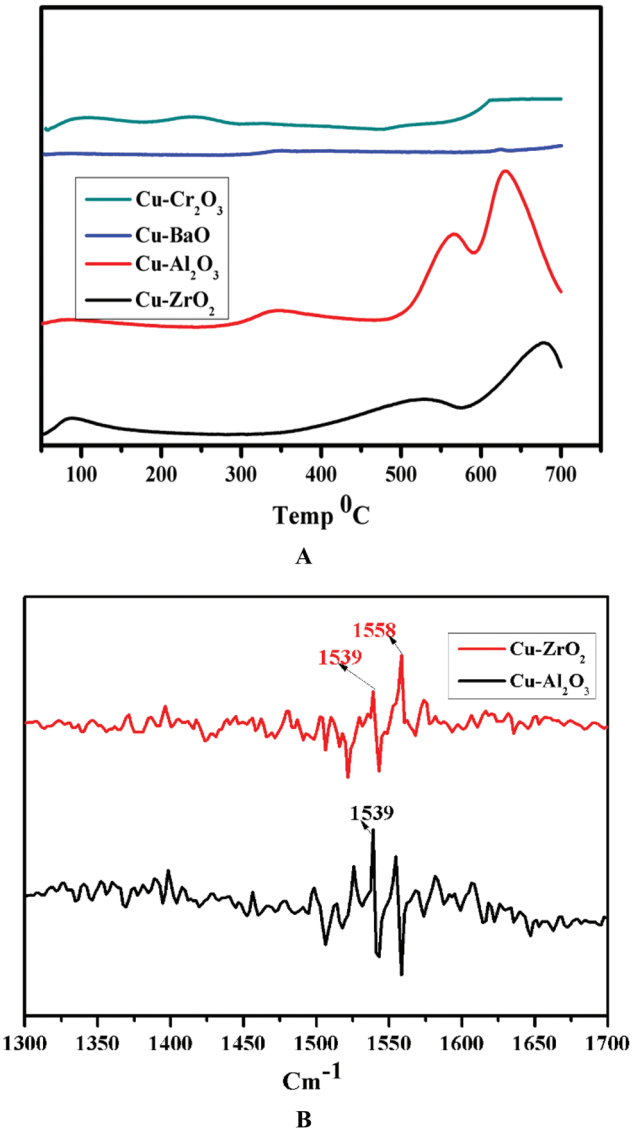

Fig. 3 NH_3-TPD and Py-IR profiles of copper based catalysts: (A) NH_3-TPD profiles of copper catalysts, and (B) pyridine-IR of copper with Al and Zr catalysts.

catalyzed esterification of LA in methanol as discussed later.[19–21]

Catalyst stability was studied by TG–DTA and the results are shown in Fig. 4(A) and (B). TG profiles of Cu–Cr_2O_3 and Cu–BaO showed the decomposition of these catalysts after 400 °C and 600 °C respectively. On the other hand, both Cu–ZrO_2 and Cu–Al_2O_3 showed excellent stability up to 700 °C. DTA of the TG profiles of all the samples (Fig. 4B) showed 8–9% weight loss around 100–120 °C, due to the loss of water molecules. The broad exothermic peaks for Cu–Cr_2O_3 and Cu–BaO catalysts could be due to the loss of Cu in the form of CuO to the extent of 30% which was much higher than that observed for Cu–ZrO_2 and Cu–Al_2O_3 (8–9%) catalysts.[22,23] This confirms the higher stability of Cu–ZrO_2 catalyst as well as retention of active Cu for higher hydrogenation activity than that of other Cu catalysts.

Fig. 5 shows the H_2 TPR of all the copper catalysts studied in this work. All the samples exhibited a broad band of H_2

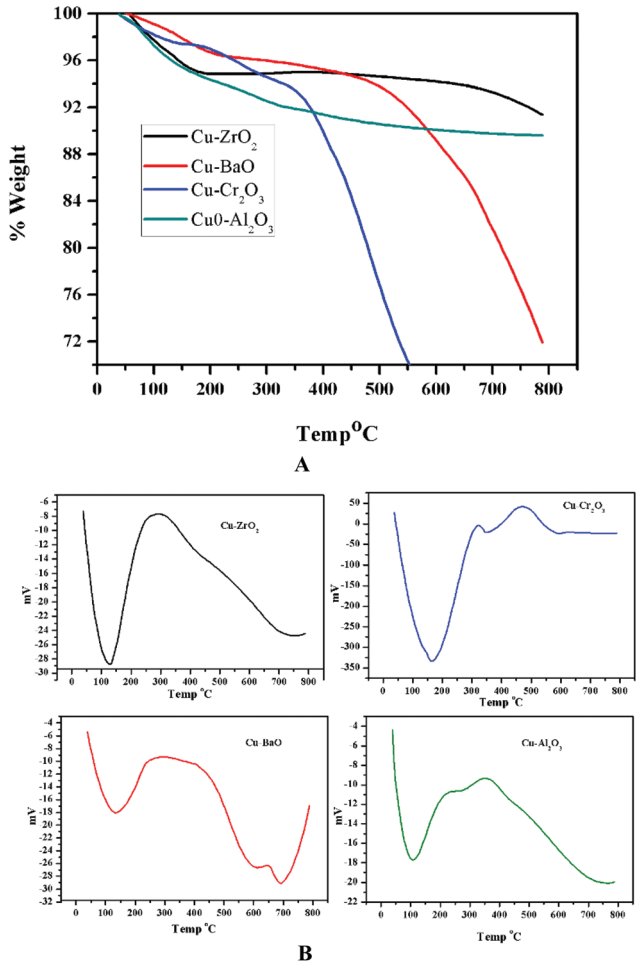

Fig. 4 TG–DTA profiles of copper based catalysts: (A) TG analysis of the copper catalysts, and (B) DTA of the copper catalysts.

consumption in the range of 180–356 °C. The shape of the H_2 consumption peak was asymmetric due to the presence of a shoulder or a tail, as a result of a complex overlapping of several elemental reduction processes such as sequential reduction of CuO to Cu^0 *via* Cu_2O.[24,25] The highest reduction temperature (359 °C) of Cu–ZrO_2 sample confirms the strong interaction of Cu and ZrO_2, contributing to its greater stability under reaction conditions.

Fig. 6(A) and (B) show HRTEM images of the Cu–ZrO_2 before and after reaction in the water medium respectively. The TEM image (Fig. 6A) shows the well dispersed nature of the Cu nanoparticles on the zirconia surface with particle sizes in the range of 10–14 nm which is close to the particle size estimated from XRD (13–14 nm).[26] HRTEM of the used Cu–ZrO_2 sample (Fig. 6B) showed minor agglomeration of Cu particles giving the particle size of 13–15 nm. The '*d*'-spacing of the used catalyst determined form the pattern of fringes (inset right bottom, Fig. 6B) was found to be 3.2 Å which was also close to that obtained by XRD (2.9 Å) for $2\theta = 43.50°$ (111) plane of metallic copper. On the contrary, fresh Cu–Al_2O_3 (Fig. 6C) showed agglomeration of the particles and did not allow to specify the fringes pattern. In case of recovered Cu–Al_2O_3 (Fig. 6D), the particles got oriented into a distinct rod like structure without any fringes. This could be due to substantial leaching of Cu, as discussed in detail later (Table 2).

The preliminary results on hydrogenation of LA to GVL using various copper catalysts in both water and methanol solvents are presented in Table 1. The desired product GVL was identified by H^1NMR, ^{13}C-NMR, DEPT and the respective spectra are given in the supporting information (ESI, Fig. 3–5†). It is interesting to note that copper in combination with Zr and Al showed complete LA conversion in water while, copper with other metals showed very poor LA conversion in the range of 4–45%, although complete GVL selectivity was obtained in all the cases. On the other

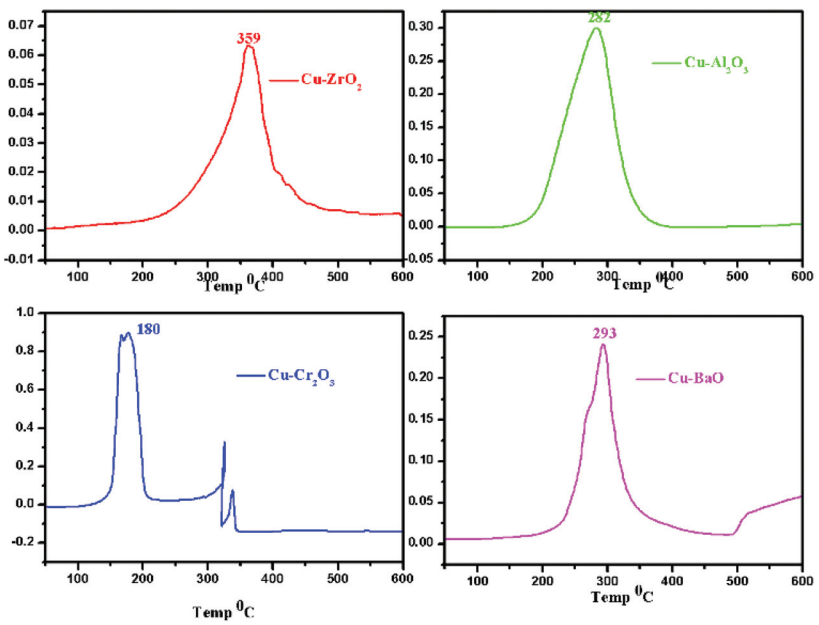

Fig. 5 H_2 TPR profiles of copper based catalysts.

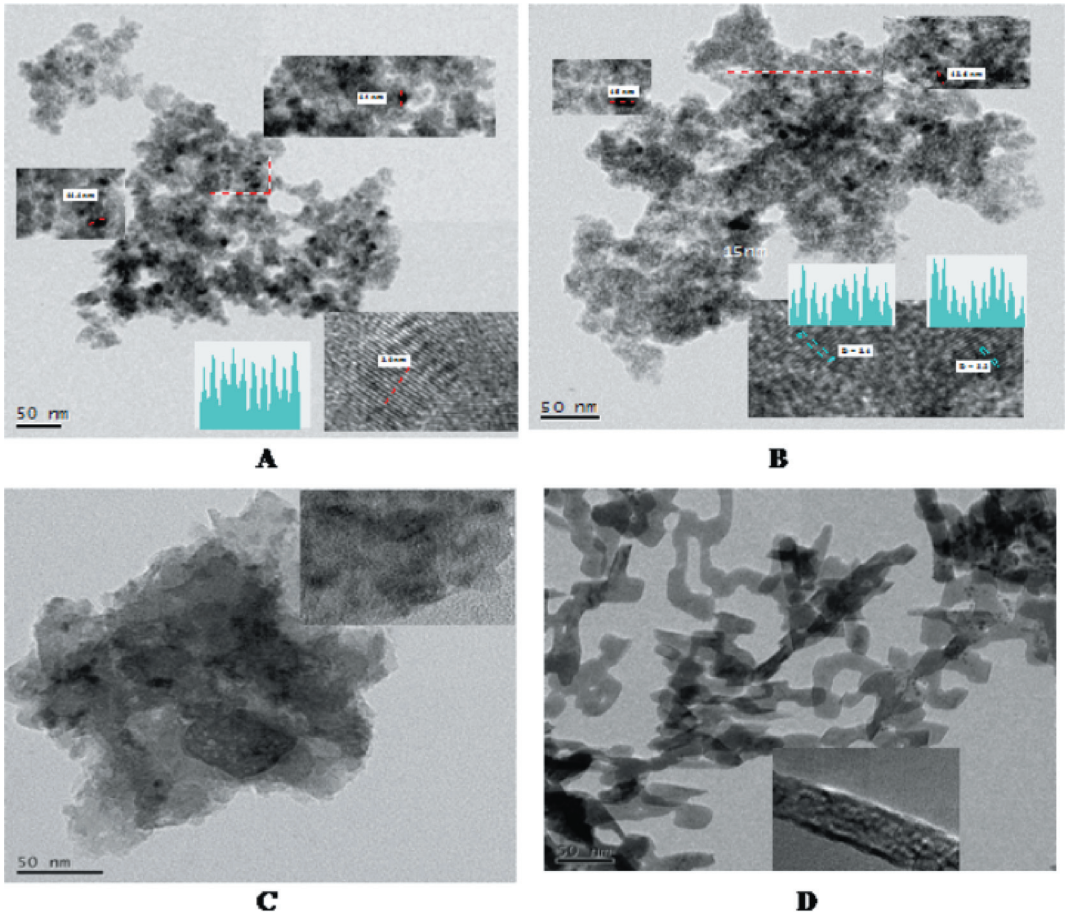

Fig. 6 HR-TEM images of the nano catalyst: (A) activated Cu–ZrO_2 catalyst; (B) used Cu–ZrO_2 catalyst in water; (C) activated Cu–Al_2O_3 catalyst; (D) used Cu–Al_2O_3 catalyst in water.

Table 1 Catalyst screening for hydrogenation of LA in water and methanol[a]

	Water		Methanol			
		Selectivity, %		Selectivity, %		
Catalysts	Conversion, %	GVL	Conversion, %	GVL	4-HMeLA	MeLA
Cu–ZrO_2 (1 : 1)	**100**	**100**	**100**	**90**	**9**	**1**
Cu–Al_2O_3 (1 : 1)	100	100	100	86	10	4
Cu–Cr_2O_3 (1 : 1)	9	100	72	45	20	35
Cu–BaO (1 : 1)	12	100	78	41	9	50
Cu–Cr_2O_3–Al_2O_3 (4 : 4 : 2)	40	100	89	82	14	2
Cu–BaO–Al_2O_3 (4 : 4 : 2)	45	100	92	86	8	6

[a] Reaction conditions: levulinic acid, 5% (w/w); solvent, water and MeOH (95 mL); temperature, 473 K; H_2 pressure, 500 psi; catalyst, 0.5 g; reaction time, 5 h.

hand, in methanol solvent, a maximum GVL selectivity of up to 90% was achieved only in the case of Cu–ZrO_2 and Cu–Al_2O_3 catalysts. Copper, in combination with other metals, gave LA conversion of <90% with GVL selectivity ranging from 45–86%. The lowering of the GVL selectivity was due to unconverted 4-HMeLA and MeLA (Scheme 1). The poor surface acidity of the Cu catalysts with metals other than Zr and Al, as evidenced by NH_3-TPD, was responsible for the slower rate of esterification (Fig. 7). This also affected the further steps of Cu catalyzed hydrogenation and acid catalyzed cyclization to GVL leading to accumulation of 4-HMeLA and MeLA. The marginal lower selectivity to GVL in methanol over Cu–ZrO_2 catalyst was due to less facile cyclization of 4-hydroxyl methyl levulinate having a bulkier methyl group as compared to that of 4-hydroxyl levulinic acid. The excellent catalytic performance of our copper–zirconia catalyst could be due to (i) its strong surface acidity that catalyzes cyclization of the intermediate hydroxyl levulinic acid–ester due to the protonation of hydroxyl group,[27]

Table 2 Catalyst activity and stability for the synthesis of GVL[a]

Catalysts	Substrate	Solvent	Conversion, %	Selectivity, %			Metal leaching (ppm)
				GVL	Me-LA	4-hydroxy Me-LA	
$Cu–ZrO_2$	Levulinic acid	Water	100	>99.9	0.01	0.01	34
	Levulinic acid	Methanol	100	90	2	8	2
	Methyl levulinate	Methanol	95	92	SM	8	ND
	Methyl levulinate[b]	Methanol	81	79	SM	21	ND
	Levulinic acid	Water	100	>99.9	0.01	0.01	174
$Cu–Al_2O_3$	Levulinic acid	Methanol	100	86	4	10	31
	Methyl levulinate	Methanol	93	88	SM	12	ND

[a] Reaction conditions: LA, MeLA, (5% w/w); temperature, 473 K; H_2 pressure, 500 psi; catalyst, 0.5 g; reaction time, 5 h. [b] Reaction conditions: methyl LA, (20% w/w); temperature, 473 K; H_2 pressure, 500 psi; catalyst, 0.5 g; reaction time, 5 h.

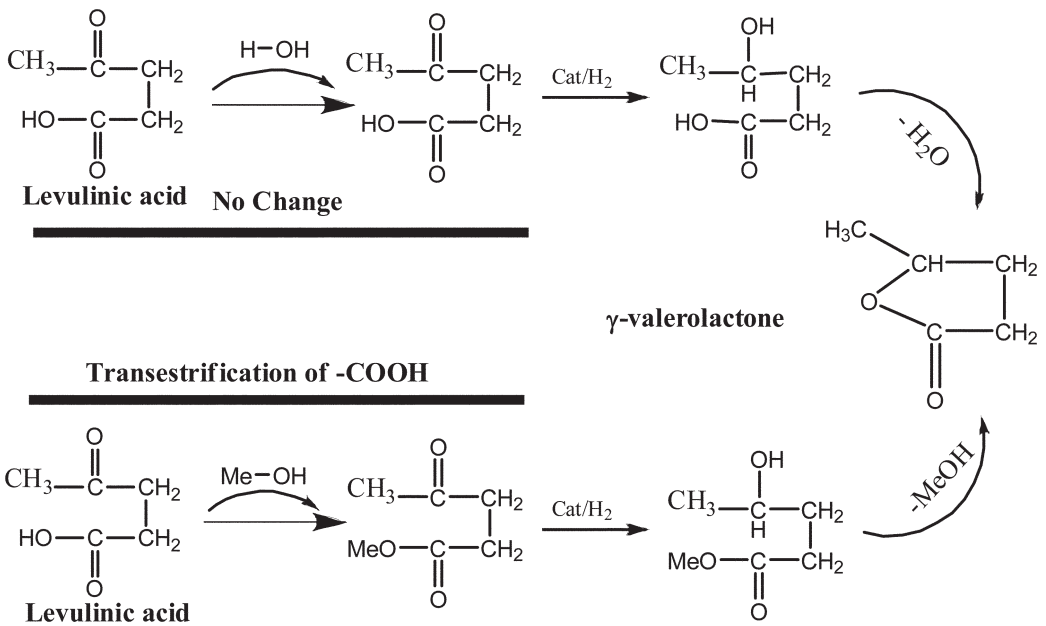

Scheme 1 Catalytic hydrogenation of levulinic acid in presence of water and methanol.

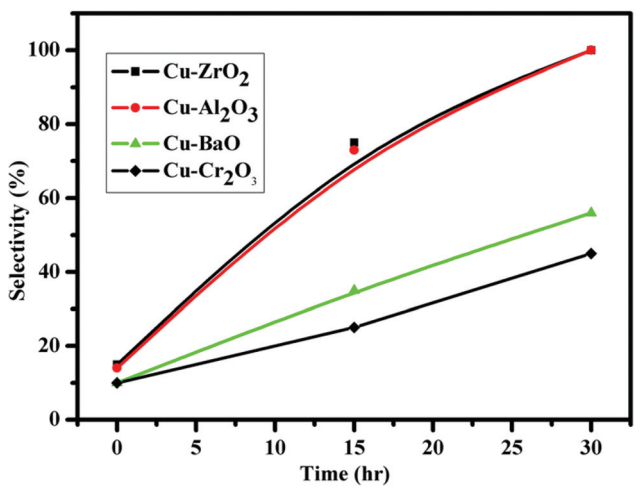

Fig. 7 Selectivity profile for methyl levulinate formation.

(ii) the microporous nature of $Cu–ZrO_2$ as evidenced by the type IV isotherm (ESI, Fig. 1, Table 1†),[28] (iii) ZrO_2 also plays a role in the first step of hydrogenation in which hydrogen adsorbs dissociatively on ZrO_2,[29] (iv) among the dopent oxides of other metals such as barium, chromium and aluminium, ZrO_2 is the most stable to "decoking" conditions during repeated catalyst regeneration cycles, and (v) ZrO_2 shows much higher stability against its leaching in aqueous LA solution in high temperature reaction conditions, as proven by the catalyst recycles studies described later.[12,13]

The role of acidity of $Cu–ZrO_2$ and $Cu–Al_2O_3$ catalyst was further studied by the kinetics of the first step esterification reaction. Fig. 7 shows selectivity *vs.* time patterns for conversion of LA to methyl levulinate over various copper based catalysts in methanol. Copper with Zr and Al gave complete formation of methyl levulinate within the first 30 min of the reaction, while other metals like Ba and Cr showed lower activity for the transesterification step. It is also interesting to note that the hydrogenation of methyl levulinate begins only after the complete formation of methyl levulinate, indicating the competitive adsorption of LA and methyl levulinate (ESI, Fig. 6A and B†).

As stability is critical for the efficient use of any catalyst, Cu metal leaching was studied for the $Cu–ZrO_2$ and $Cu–Al_2O_3$

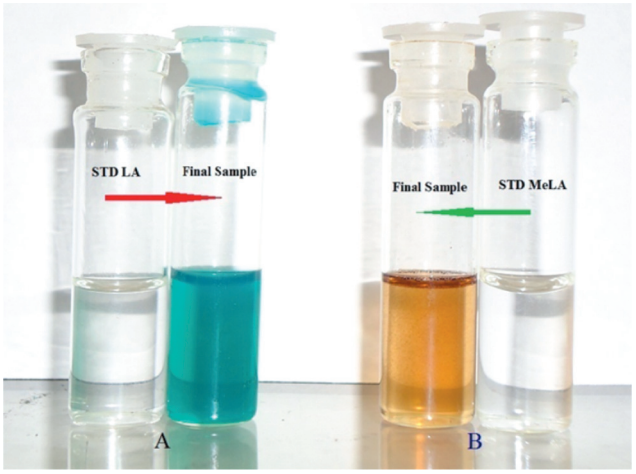

Fig. 8 Final reaction sample of LA hydrogenation in water and methanol (A) final reaction sample of LA in water with Cu–Al_2O_3 catalyst (B) final reaction sample of MeLA in methanol with Cu–ZrO_2 catalyst. Levulinic acid, 5% (w/w); solvent, water, methanol (95 mL); temp, 473 K; catalyst, 0.5 g; (Cu–Al_2O_3, Cu–ZrO_2) reaction time, 5 h.

catalysts since almost complete conversion of LA with similar selectivities to GVL were obtained for both catalysts. The extent of Cu metal leaching was dramatically affected by the change in the reaction medium. As can be seen from Table 2, the active metal leaching was maximum (174 ppm) for the Cu–Al_2O_3 catalyst while it was only 34 ppm in case of the Cu–ZrO_2 catalyst in the water medium. Even in methanol solvent, metal leaching up to 31 ppm was observed for Cu–Al_2O_3 while it was almost completely suppressed in the case of the Cu–ZrO_2 catalyst. However, for the Cu–ZrO_2 catalyst no metal leaching was observed when methyl levulinate was used as a substrate in spite of the substrate loading being increased from 5 to 20% w/w. Copper metal leaching was evident visibly by observing the blue colour of the crude reaction in the case of the Cu–Al_2O_3 catalyzed reaction (Fig. 8). The blue colour of the solution was due to the formation of a soluble metal carboxylate complex with levulinic acid.[30] This was also confirmed by FT-IR (ESI, Fig. 7A and B†) in which the frequency of the carbonyl group of levulinic acid shifted from 1702 cm^{-1} to 1565 cm^{-1}, while no change was observed for methyl levulinate as a substrate.[30] Thus metal leaching could be avoided at least in the case of Cu–ZrO_2 in the presence of methanol, where the carboxyl group undergoes transesterification thus rendering the free carboxylic group unavailable, so cannot form a soluble copper complex.[30] The proposed reaction mechanism as shown in Scheme 1, is believed to proceed differently in methanol than in water. In the presence of methanol the first step of the transesterification of the carboxyl group forms methyl levulinate and its subsequent hydrogenation to GVL involves the elimination of methanol, which can be recycled. On the other hand, in water the first step is the direct hydrogenation of the keto group to give 4-hydroxy levulinic acid followed by its dehydration to give cyclic GVL.

The catalyst reuse studies for Cu–ZrO_2 catalyst were carried out as follows. After the first hydrogenation was complete, the reaction crude was allowed to settle down and supernatant clear product mixture was removed from the reactor. A fresh charge of reactants was added to the catalyst residue retained in the reactor

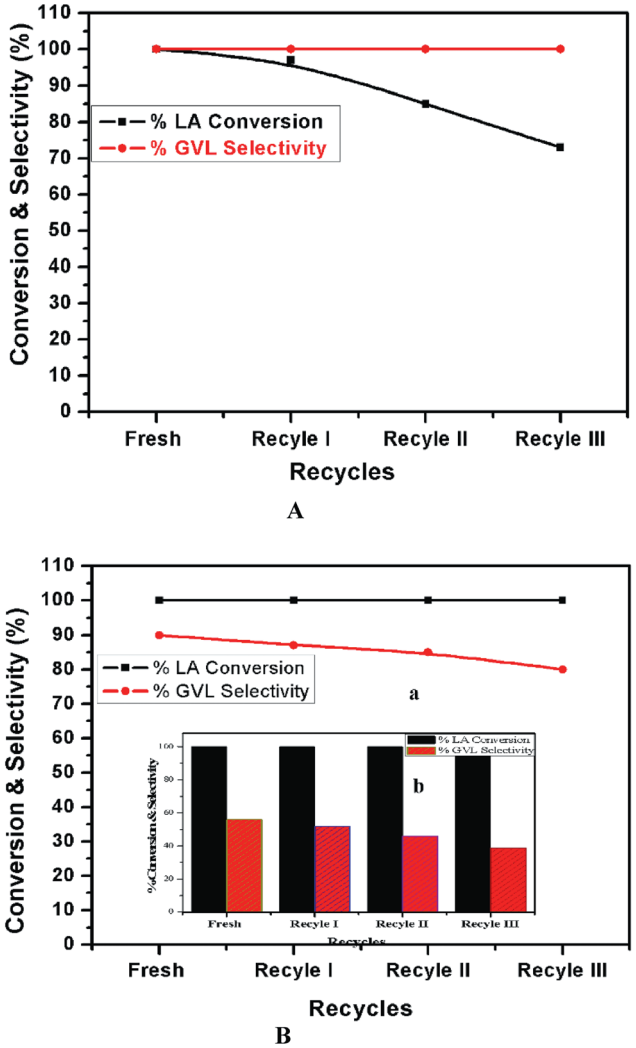

Fig. 9 Recycling study of LA hydrogenation: (A) conversion and selectivity pattern of LA hydrogenation in water; (B) conversion and selectivity pattern of LA hydrogenation in methanol, (a) 0.500 mg catalyst loading, and (b) 0.150 mg catalyst loading.

and the subsequent run was continued. This procedure was followed for three subsequent runs and the results are shown in Fig. 9(A) and (B). Our copper zirconia catalyst showed almost the same activity with slight decrease in selectivity for LA hydrogenation in methanol even after the third recycle. A marginal decrease in selectivity from 90 to 80% could be due to sintering of the active sites of metal particles. The reuse of copper zirconia catalyst was also demonstrated with a lower catalyst loading of 0.15 g which gave consistent activity as indicated by complete conversion after the third recycle. The catalyst activity dropped down to 70% in an aqueous medium due to copper leaching in the reaction crude (Table 2).

Experimental procedure

Materials

Levulinic acid (99%) and methyl levulinate were purchased from Sigma-Aldrich, Bangalore, India while, methanol (>99.9%) was

purchased from Rankem, India. Copper nitrate and zirconium nitrate were purchased from Loba Chemie, Mumbai, India. Hydrogen (>99.99%) purity was obtained from Inox, India.

Catalyst preparation

The copper–zirconia (Cu–ZrO_2) catalyst was prepared by the co-precipitation method in which 0.05 M aqueous solutions of Cu $(NO_3)_2{\cdot}3H_2O$ and $Zr(NO_3)_3{\cdot}3H_2O$ were taken and precipitated using 0.2 M aqueous potassium carbonate at room temperature. The precipitate was aged further for 6 h at room temperature. Then the precipitate was separated by filtration and washed with deionized water to remove the traces of potassium. The precipitate thus obtained, was dried in static air oven at 373 K for 8 h and calcined at 673 K for 4 h. Prior to the reaction, the calcined catalyst was reduced in H_2 pressure.

All other copper catalysts tested in this work (Cu–Al_2O_3, Cu–BaO, Cu–Cr_2O_3, Cu–Cr_2O_3–Al_2O_3, Cu–BaO–Al_2O_3) were prepared by using a co-precipitation method. In a typical preparation, 0.5 M of each of $Cu(NO_3)_2{\cdot}3H_2O$ and the other metal nitrate in case of two component system, while 0.4 M of each of Cu $(NO_3)_2$ nitrate precursors of the respective metals (Al, Cr and Ba) in case of tricomponents, were dissolved in deionized water and precipitated using 0.2 M aqueous potassium carbonate at room temperature. The precipitate was aged further for 6 h at room temperature. Then the precipitate was separated by filtration and washed with deionized water to remove the traces of potassium. The precipitate thus obtained was dried in static air oven at 373 K for 8 h and calcined at 673 K for 4 h. Prior to the reaction, the calcined catalyst was reduced in H_2 flow.

Hydrogenation experiments and analysis

LA hydrogenation reactions were carried out in a 300 mL capacity autoclave (Parr Instruments Co., USA) at a stirring speed of 1000 rpm. The typical hydrogenation conditions were: temperature, 473 K; LA concentration, 5 wt%; solvent, 95 mL; total volume, 100 mL; catalyst loading, 0.5 g; substrate : catalyst mole ratio, (10 : 1) and hydrogen pressure, 3–4 MPa. The catalysts were pre-reduced under H_2 at 573 K for 12 h. and then stored in a vacuum desiccator. Liquid samples were withdrawn periodically and analyzed by GC (HP-6890) having HP-5 column with FID detector.

Catalyst characterization

X-Ray diffraction patterns were recorded on a PAnalytical PXRD Model X-Pert PRO-1712, using Ni filtered Cu Kα radiation (λ = 0.154 nm) as a source (current intensity, 30 mA; voltage, 40 kV) and X-celerator detector. The samples were scanned in the 2θ range of 20–80°.

The crystallite size was determined by Scherrer equation.

$$D = k\lambda/\beta\mathrm{Cos}\theta$$

The Raman spectra of sample were recorded on a Horiba JY Lab RAM HR800 micro-Raman spectrometer with 17 mW, 632.8 nm laser excitation.

NH_3-TPD experiments were carried out on a Chemisoft TPx (Micromeritics-2720) instrument. In order to evaluate acidity of the catalysts, ammonia TPD measurements were carried out by: (i) pre-treating the samples from room temperature to 300 °C under a helium flow rate of 25 mL min^{-1}, (ii) adsorption of ammonia at 50 °C, (iii) desorption of ammonia with a heating rate of 10 °C min^{-1} starting from the adsorption temperature to 973 K. Py-IR spectra were recorded on shimadzu FTIR 8000 attached with SSU (second sampling unit) using 20 mg catalyst sample. Sample was filled in a sample cup, 20 mL of pyridine were injected in N_2 flow. FTIR spectra were recorded on a Perkin-Elmer instrument. The pellets for analysis were prepared by mixing 2 mg of the catalyst with 150 mg of KBr. FTIR spectra were recorded between 400 and 4000 cm^{-1} with accumulation of 20 scans and 4 cm^{-1} resolution.

Thermogravimetric analysis (TG–DTA) was performed on Perkin-Elmer TGA-7 analyzer at a 10 °C min^{-1} scan rate in nitrogen atmosphere starting from room temperature to 800 °C.

TPR experiments of the prepared copper catalysts were also performed on a Chemisoft TPx (Micromertics-2720). In the TPR experiment, a U-tube (quartz tube) was filled with solid catalyst. This sample holder was positioned in a furnace equipped with a temperature control. A thermocouple was placed in the solid for temperature measurement. Equal quantity of fresh vacuum dried catalyst was taken in the U-tube. Initially, flow of inert gas (argon) was passed through U-tube to remove the air present in the lines, and heated in Ar atmosphere with a flow rate of 25 mL min^{-1} to 200 °C for 30 min to remove the moisture and surface impurities present on the sample and then it was cooled to room temperature. Ar was replaced by a mixture of 5% H_2 in Ar gas for the TPR experiment with a heating rate of 10 °C min^{-1} starting from the room temperature to 700 °C and a thermal conductivity detector (TCD) measured the hydrogen uptake.

The particle size and morphology were studied using transmission electron microscope (HR-TEM), model JEOL 1200 EX. A small amount of the solid sample was sonicated in 2-propanol for 1 min. A drop of prepared suspension was deposited on a Cu grid coated with a carbon layer, the grid was then dried at room temperature before analysis. The sample analysis of metal leaching experiments was carried out by using instrument (ICP-OES), the supernatant liquid was evaporated and resulting solid was treated with *aqua regia* (HNO_3 : HCl = 1 : 3), 60 °C on a sand bath for 2 h and than made up to 25 mL by distilled water.

Conclusion

Non-noble metal nanocomposite catalysts were developed for the first time by incorporating Zr and Al with copper, for selective hydrogenation of levulinic acid and its methyl ester to GVL. HRTEM revealed the particle size of copper in a range of 10–14 nm. Both XRD and Raman spectroscopy confirmed the formation of the Cu–ZrO_2 nanocomposite and also the presence of mixed oxide phases along with Cu^0. Both the catalysts showed complete conversion of LA and its ester with >90% selectivity to GVL. Interestingly, for LA hydrogenation in methanol only Cu–ZrO_2 could be recycled efficiently four times, with almost no leaching of the active metal. In methanol, the hydrogenation was found to proceed *via* the first step of the

transesterification to the corresponding ester followed by its *in situ* hydrogenation to GVL.

Abbreviations

GVL	γ-valerolactone
LA	levulinate or levulinic acid
MeLA	methyl levulinate
4-MeLA	4-hydroxy methyl levulinate

Acknowledgements

One of the authors, AMH thanks the Council of Scientific and Industrial Research (CSIR) New Delhi, for the award of a senior research fellowship.

References

1 M. J. Climent, A. Corma and S. Iborra, *Green Chem.*, 2011, **13**, 520–540.
2 J. J. Bozell and G. R. Petersen, *Green Chem.*, 2010, **12**, 539–554.
3 I. T. Horvath, H. Mehdi, V. Fabos, L. Boda and L. T. Mika, *Green Chem.*, 2008, **10**, 238–242.
4 G. W. Huber, S. Iborra and A. Corma, *Chem. Rev.*, 2006, **106**, 4044–4098.
5 E. Manzer, *Appl. Catal., A*, 2004, **272**, 249–256.
6 J. P. Lange, J. Z. Vestering and R. J. Haan, *Chem. Commun.*, 2007, 3488–3490.
7 C. V. Bylandtlaan, *WO*, 099111, 2007.
8 R. W. Christian, H. D. Brown and R. M. Hixon, *J. Am. Chem. Soc.*, 1947, **69**, 1961–1962.
9 H. A. Schutte and R. W. Thomas, *J. Am. Chem. Soc.*, 1930, **52**, 3010–3012.
10 R. A. Bourne, J. G. Stevens, J. Ke and M. Poliakoff, *Chem. Commun.*, 2007, 4632–4634.
11 Z. P. Yan, L. Lin and S. J. Liu, *Energy Fuels*, 2009, **23**, 3853–3858.
12 J. P. Lange, R. Price, P. M. Ayoub, J. Louis, L. Petrus, L. Clarke and H. Gosslink, *Angew. Chem., Int. Ed.*, 2010, **49**, 4479–4483.
13 R. J. Hann and J. P. Lange, *US*, 0046399, 2011.
14 D. J. Braden, C. A. Henao, J. Heltzel, C. C. Maravelias and J. A. Dumesic, *Green Chem.*, 2011, **13**, 1755–1765.
15 L. Deng, Y. Zhao, J. Li, Y. Fu, B. Liao and Q. X. Guo, *ChemSusChem*, 2010, **3**, 1172–1175.
16 X. L. Du, L. He, S. Zhao, Y. M. Liu, H. Y. He and K. N. Fan, *Angew. Chem., Int. Ed.*, 2011, 50, 7815–7819.
17 D. J. Li, D. M. Lai, Y. Fu and Q. X. Guo, *Angew. Chem., Int. Ed.*, 2009, **48**, 6529–6532.
18 X. Hu and C. Z. Li, *Green Chem.*, 2011, **13**, 1676–1679.
19 L. Wang, W. Zhu, D. Zheng, X. Yu, J. Cui, M. Jia, W. Zhang and Z. Wang, *React. Kinet., Mech. Catal.*, 2010, **101**, 365–375.
20 L. C. Wang, Q. Liu, M. Chen, Y. M. Liu, Y. Cao, H. Y. He and K. N. Fan, *J. Phys. Chem. C*, 2007, **111**, 16549–16557.
21 K. V. R. Chary, K. K. Seela, D. Naresh and P. Ramakanth, *Catal. Commun.*, 2008, **9**, 75–81.
22 Y. Wang and R. A. Caruso, *J. Mater. Chem.*, 2002, **12**, 1442–1445.
23 M. K. Dongare, A. M. Dongare, V. B. Tare and E. Kemnitz, *Solid State Ionics*, 2002, **152–153**, 455–462.
24 C. Z. Yao, L. C. Wang, Y. M. Liu, G. S. Wu, Y. Cao, W. L. Dai, H. Y. He and K. N. Fan, *Appl. Catal., A*, 2006, **297**, 151–158.
25 Z. HY, Z. YL, H. L, Z. ZY, W. HJ and L. YW, *Catal. Commun.*, 2008, **9**, 342–348.
26 X. Guo, D. Mao, G. Lu, S. Wang and G. Wu, *Catal. Commun.*, 2011, **12**, 1095–1098.
27 K. Arata, *Green Chem.*, 2009, **11**, 1719–1728.
28 S. Xie, E. Iglesia and A. T. Bell, *Chem. Mater.*, 2000, **12**, 2442–2445.
29 J. Wambach, A. Baikerb and A. Wokaun, *Phys. Chem. Chem. Phys.*, 1999, **1**, 5071–5080.
30 L. Chen, H. Meng, L. Jiang and S. Wang, *Chem.–Asian J.*, 2011, **6**, 1757–1760.

